bridged, dative metal-metal bonds (i.e., Os→Os→W), is a remarkably stable molecule.[7] The X-ray structure of the compound reveals that the sterically undemanding P(OCH$_2$)$_3$CMe ligands[35] occupy positions that are mutually trans but are also cis to the Os-Os dative bond.[7] It thus appears that, for compounds of the type Os(CO)$_{5-x}$(L)$_x$ (x = 1, 2) to be good donor ligands, L should be a good σ-donor ligand and small so that it can occupy a site cis to the dative metal-metal bond.

(35) Tolman, C. A. *Chem. Rev.* **1977**, *77*, 313.
(36) Carruthers, J. R.; Watkin, D. J. *Acta Crystallogr., Sect. A: Cryst. Phys., Diffr., Theor. Gen. Crystallogr.* **1979**, *A35*, 698.

Acknowledgment. We thank the Natural Sciences and Engineering Research Council of Canada for financial support. We also thank Professor J. Takats (University of Alberta) for a copy of Dr. M. R. Burke's Ph.D. thesis.

Supplementary Material Available: Figures of the carbonyl region of the ^{13}C NMR spectrum of **1-Cr**, **1-Mo**, and **1-W** and the carbonyl region of the ^{13}C NMR spectrum of **2a-Cr**, **2a-Mo**, and **2a-W**, a listing of supplementary crystallographic data for **1-Cr** and **2b-Cr**, and tables of hydrogen atom coordinates and anisotropic temperature factors for **1-Cr** and **2b-Cr** (6 pages); listings of observed and calculated structure factors for **1-Cr** and **2b-Cr** (25 pages). Ordering information is given on any current masthead page.

Synthesis and Carbonyl Exchange in (η^5-C$_5$R$_5$)(OC)Ir[Os(CO)$_4$]$_2$ (R = H, Me). Structure of (η^5-C$_5$Me$_5$)(OC)Ir[Os(CO)$_4$]$_2$

Andreas Riesen, Frederick W. B. Einstein, Andrew K. Ma, Roland K. Pomeroy,* and John A. Shipley

Department of Chemistry, Simon Fraser University, Burnaby, British Columbia, Canada V5A 1S6

Received September 25, 1990

The clusters (η^5-C$_5$R$_5$)(CO)Ir[Os(CO)$_4$]$_2$ (R = H, **1**; R = Me, **1***) were isolated (28% yield) as air-stable, red crystals from the reaction of (η^5-C$_5$R$_5$)Ir(CO)$_2$ and Os(CO)$_4$(η^2-cyclooctene) in hexane at 55-65 °C. The structure of **1*** has been determined by X-ray crystallography: space group $P\bar{1}$ with a = 9.107 (3) Å, b = 9.128 (2) Å, c = 14.639 (2) Å, α = 84.63 (1)°, β = 78.96 (2)°, γ = 66.90 (2)°, Z = 2, R = 0.030, R_w = 0.040 for 3738 reflections ($I \geq 2.5\sigma(I)$). The structure consists of an Ir(η^5-C$_5$Me$_5$)(CO) and two Os(CO)$_4$ units bound in a triangular array (Ir-Os(1) = 2.7902 (5), Ir-Os(2) = 2.8124 (5), Os(1)-Os(2) = 2.8536 (5) Å); the carbonyl ligand bound to the iridium atom occupies an axial site. The ^{13}C NMR spectrum of **1** in CH$_2$Cl$_2$/CD$_2$Cl$_2$ at -48 °C exhibits five sharp carbonyl resonances in the ratio 2:2:1:2:2 consistent with a rigid structure similar to that of **1*** in the solid state. On warming the sample to +7 °C, four of the carbonyl resonances collapsed to the base line. This mode of collapse is interpreted in terms of partial merry-go-round CO exchanges that occur in the two planes that are perpendicular to the plane of the metal atoms and pass through the Ir and one of the Os atoms. Simulation of the spectrum at -10 °C indicated $\Delta G^{\ddagger}$ = 14.2 kcal mol^{-1} for the barrier to the exchange. Cluster **1*** exhibited similar behavior but with a much lower activation energy for the CO exchange: $\Delta G^{\ddagger}$ = 7.4 kcal mol^{-1} (from the simulation of the spectrum at -116 °C).

Introduction

One of the fascinating properties of metal carbonyl clusters is the stereochemical nonrigidity they often exhibit.[1,2] A number of different types of CO exchange have been identified, and plausible mechanisms have been proposed for these processes. It is still not clear, however, why one process has a low activation barrier whereas another, which superficially resembles the first, has a much higher barrier.

We have recently described the synthesis and structure of the triangular cluster (OC)$_5$Cr[Os(CO)$_3$(PMe$_3$)]$_2$.[3] The ^{13}C NMR spectrum of this cluster in solution at -122 °C had carbonyl resonances that were consistent with the presence of two isomers, and in each isomer the four radial carbonyls of the Cr(CO)$_5$ unit were equivalent but not equivalent to the axial carbonyl. The latter observation was taken to indicate that there was rapid rotation of the Cr(CO)$_5$ unit about an axis that passes through the Cr atom and the midpoint of the Os$_2$ vector.[3] At higher temperatures, the spectra of each isomer underwent changes consistent with at least two other types of carbonyl exchange. The molybdenum and tungsten analogues of (OC)$_5$Cr[Os(CO)$_3$(PMe$_3$)]$_2$ behaved similarly.[4]

The triosmium cluster (OC)$_4$Os{Os(CO)$_3$[P(OMe)$_3$]}$_2$ also exhibits ^{13}C NMR signals, in solution at -66 °C, consistent with the presence of two isomers analogous to those of (OC)$_5$Cr[Os(CO)$_3$(PMe$_3$)]$_2$.[5] The Os(CO)$_4$ units in each isomer are, however, rigid. Indeed, one carbonyl resonance

(1) (a) Band, E.; Muetterties, E. L. *Chem. Rev.* **1978**, *78*, 639. (b) Geoffroy, G. L. *Acc. Chem. Res.* **1980**, *13*, 469. (c) Johnson, B. F. G.; Benfield, R. E. In *Transition Metal Clusters*; Johnson, B. F. G., Ed.; Wiley: Chichester, England, 1980; p 471.
(2) (a) Mann, B. E. In *Comprehensive Organometallic Chemistry*; Wilkinson, G., Stone, F. G. A., Abel, E. W., Eds.; Pergamon: New York, 1982; Vol. 3, p 89. (b) Deeming, A. J. *Adv. Organomet. Chem.* **1986**, *26*, 1.
(3) Davis, H. B.; Einstein, F. W. B.; Johnston, V. J.; Pomeroy, R. K. *J. Am. Chem. Soc.* **1988**, *110*, 4451.
(4) Davis, H. B.; Pomeroy, R. K. To be submitted for publication.
(5) Alex, R. F.; Pomeroy, R. K. *Organometallics* **1987**, *6*, 2437.

0276-7333/91/2310-3629$02.50/0

attributed to an equatorial carbonyl of the $Os(CO)_4$ unit of the less symmetric isomer remains sharp in the spectrum at −3 °C (at higher temperatures, all the remaining sharp signals collapsed to the base line).[5] There is, therefore, a large difference in the ease of rotation of the formally isolobal[6] fragments $M(CO)_5$ (M = Cr, Mo, W) and $Os(CO)_4$ in trinuclear clusters.

It is of interest to investigate the possible rotation of other organometallic fragments that are isolobal with $Os(CO)_4$ in trinuclear clusters that have two $Os(CO)_3(L)$ (L = two-electron donor ligand) groups. One such fragment is $M'(\eta^5\text{-}C_5R_5)(CO)$ (M' = Rh or Ir; R = H or Me). Shore and co-workers have reported the preparation and variable-temperature ^{13}C NMR spectra of $(\eta^5\text{-}C_5H_5)(OC)Rh[Os(CO)_4]_2$ (**1-Rh**).[7] However, even with the sample at −95 °C, other carbonyl-exchange processes were still rapid on the NMR time scale. Recently Washington and Takats[8] have described an alternative synthesis of **1-Rh**, and the synthesis $(\eta^5\text{-}C_5Me_5)(OC)Rh[Os(CO)_4]_2$ (**1*-Rh**). Furthermore, they observed a dramatic increase in the barrier to carbonyl exchange on going from **1*-Rh** to **1-Rh** as monitored by ^{13}C NMR spectroscopy. The spectrum of **1-Rh** in THF-d_8 at −115 °C was consistent with a rigid structure that was similar to the structure in the solid state; that is, the $Rh(\eta^5\text{-}C_5H_5)(CO)$ group was rigid with respect to the rest of the molecule (except, of course, for the rotation of the C_5H_5 ligand).

Our strategy has been the synthesis of the iridium analogues of **1-Rh** and **1*-Rh** (**1** and **1***, respectively). This is because it is generally found in metal carbonyl clusters that the barriers to carbonyl exchange increase on going to the metal lower in the periodic table. Herein, we describe the preparation of **1** and **1*** along with the crystal structure of the latter cluster. We also report the variable-temperature ^{13}C NMR studies on these clusters that essentially confirm the results of Washington and Takats. However, because of the higher barriers to CO exchange in the iridium clusters, a ^{13}C NMR spectrum of **1*** has been obtained that is close to that expected for the rigid structure.

Experimental Section

Unless otherwise stated, manipulations of starting materials and products were carried out under a nitrogen atmosphere with the use of standard Schlenk techniques. Hexane, tetrahydrofuran (THF), and dichloromethane were distilled from potassium, potassium benzophenone ketyl, and P_2O_5, respectively. Dicarbonylcyclopentadienyliridium, $(\eta^5\text{-}C_5H_5)Ir(CO)_2$, was prepared from $[Ir(CO)_3(Cl)]_n$ and TlC_5H_5;[9] the method of Maitlis[10] was used to synthesize $(\eta^5\text{-}C_5Me_5)Ir(CO)_2$ with the exception that $[(\eta^5\text{-}C_5Me_5)Ir(Cl)_2]_2$ was prepared with the use of pentamethylcyclopentadiene.[9] Other reagents were available commercially.

Infrared spectra were recorded on a Perkin-Elmer 983 spectrometer; the internal calibration of the instrument was checked against the known absorption frequencies of gaseous CO. The ^1H NMR spectra were recorded on a Bruker SY-100 NMR spectrometer. The ^{13}C NMR spectra were obtained with a Bruker WMX400 NMR spectrometer (operating frequency: 100.6 MHz) on ^{13}CO-enriched samples (~30% ^{13}C). The ^{13}CO-enriched samples were synthesized from ^{13}CO-enriched $Os_3(CO)_{12}$ that had been prepared by heating $Os_3(CO)_{12}$ in toluene at 125 °C under ~1.5 atm of ^{13}CO (99% ^{13}C) for 3 days. The NMR line-shape simulations shown in Figure 3 were carried out with a computer program written by Professor R. E. D. McClung of the University of Alberta. The electron impact (70-eV) mass spectra were obtained with a Hewlett-Packard 5985 GC–MS instrument; the pattern of the ions at highest mass in each spectrum matched that calculated for the parent ion of the compound in question. Microanalyses were performed by M. K. Yang of the Microanalytical Laboratory of Simon Fraser University.

Preparation of $(\eta^5\text{-}C_5H_5)(OC)Ir[Os(CO)_4]_2$ (1). A modified procedure of that of Burke[11] was used to prepare $Os(CO)_4(\eta^2$-cyclooctene): A Carius tube fitted with a Teflon valve was charged with $Os_3(CO)_{12}$ (50 mg, 0.055 mmol), cyclooctene (0.68 mL, 5.2 mmol), and hexane (45 mL). The tube was cooled to −196 °C and evacuated; the solution was degassed with one freeze–pump–thaw cycle. The vessel was pressurized with CO (1 atm). The stirred solution was irradiated with a Hanovia 200-W ultraviolet lamp through a GWV filter ($\lambda \geq 370$ nm). After 7 h of irradiation, the solution was filtered and transferred to a round-bottom flask (~80 mL of volume, fitted with a Teflon valve). The hexane and excess cyclooctene were removed on the vacuum line. The residue that contained the $Os(CO)_4(\eta^2$-cyclooctene) was suspended in hexane (30 mL) and $(\eta^5\text{-}C_5H_5)Ir(CO)_2$ (21 mg, 0.075 mmol) was added. The vessel was cooled to −196 °C and evacuated; the solution was degassed with one freeze–pump–thaw cycle. The flask was wrapped in aluminum foil and heated at 55–65 °C for 25 h. After this treatment, the initially pale yellow solution had become pale red. The solvent was removed on the vacuum line and the residue extracted with hexane (4 × 2 mL). The extracts were filtered (which removed most of the $Os_3(CO)_{12}$, the other major product). The extracts were combined and the solvent was removed on the vacuum line. The remaining solid was subjected to sublimation (0.1 mm) at 55–65 °C, which removed unreacted $(\eta^5\text{-}C_5H_5)Ir(CO)_2$. The solid that remained after this treatment was chromatographed on silica gel (10 × 1 cm). Elution with hexane gave a yellow band followed by an orange-red band of the desired product. The latter band was collected and the solvent removed on the vacuum line to give $(\eta^5\text{-}C_5H_5)(OC)Ir[Os(CO)_4]_2$ (21 mg, 28% based on the $Os_3(CO)_{12}$ used). The analytical sample was recrystallized from toluene to give red, air-stable crystals of **1**: IR (hexane) ν(CO) 2108 (m), 2062 (s), 2028 (s), 2013 (vs), 1995 (s), 1983 (m), 1957 (m) cm^{-1}; MS (EI), m/z 890 (M^+); ^1H NMR ($CDCl_3$) δ 5.45 (s); ^{13}C NMR (CH_2Cl_2/CD_2Cl_2, 4/1; CO region, −48 °C) δ 185.3 (2 C), 183.4 (2 C), 174.3 (1 C), 169.9 (2 C), 169.1 (2 C). Anal. Calcd for $C_{14}H_5IrO_9Os_2$: C, 18.90; H, 0.57. Found: C, 19.14; H, 0.56.

The synthesis of $(\eta^5\text{-}C_5Me_5)(OC)Ir[Os(CO)_4]_2$ (**1***) followed a similar procedure. The yield starting with 105 mg (0.116 mmol) of $Os_3(CO)_{12}$ and 50 mg (0.140 mmol) of $(\eta^5\text{-}C_5Me_5)Ir(CO)_2$ was 45 mg (27%). The analytical sample (as red, air-stable crystals) was obtained by recrystallization from hexane: IR (hexane) ν(CO) 2099 (m), 2053 (s), 2019 (vs), 2007 (vs), 2000 (sh), 1985 (s), 1973 (m), 1944 (m) cm^{-1}; MS (EI), m/z 960 (M^+); ^1H NMR ($CDCl_3$) δ 2.11 (s); ^{13}C NMR ($CHFCl_2/CD_2Cl_2$, CO region, −129 °C) δ 185.9, 179.1, 173.3, 170.2. Anal. Calcd for $C_{19}H_{15}IrO_9Os_2$: C, 23.77; H, 1.58. Found: C, 23.99; H, 1.64.

X-ray Analysis of 1*. A crystal was sealed in a glass capillary and mounted on an Enraf-Nonius CAD4 diffractometer. Cell parameters were determined from 25 accurately centered reflections in the range $30 < 2\theta < 46°$ at −78 °C. The crystal data and data collection parameters are given in Table I. Two intensity standards were measured every hour of the data acquisition time and decayed systematically by 15%. The data were corrected analytically for absorption (τ ranged from 0.024 to 0.111, checked against ψ-scan measurements).[12] Data reduction was performed including intensity scaling and Lorentz and polarization corrections.

The structure was solved from the Patterson map and subsequent Fourier series. Final full-matrix least-squares refinement included coordinates for all non-hydrogen atoms and anisotropic temperature factors for all non-hydrogen atoms except the carbonyl carbon atoms, which were refined isotropically. The hydrogen atoms were included in calculated positions and were refined together with the respective carbon atoms as rigid groups. The maximum shift/esd ratio was smaller than 0.01 for the final

(6) Hoffmann, R. *Angew. Chem., Int. Ed. Engl.* **1982**, *21*, 711.
(7) Hsu, L.-Y.; Hsu, W.-L.; Jan, D.-Y.; Marshall, A. G.; Shore, S. G. *Organometallics* **1984**, *3*, 591.
(8) Washington, J.; Takats, J. *Organometallics* **1990**, *9*, 925.
(9) Hoyano, J. K.; Graham, W. A. G. Personal communication.
(10) Kang, J. W.; Moseley, K.; Maitlis, P. M. *J. Am. Chem. Soc.* **1969**, *91*, 5970. See also: Ball, R. G.; Graham, W. A. G.; Heinekey, D. M.; Hoyano, J. K.; McMaster, A. D.; Mattson, B. M.; Michel, S. T. *Inorg. Chem.* **1990**, *29*, 2023.
(11) Burke, M. R. Ph.D. Thesis, University of Alberta, 1987.
(12) DeMeulenaer, J.; Tompa, H. *Acta Crystallogr.* **1965**, *19*, 1014.

Table I. Crystallographic Data for the Structure Determination of $(\eta^5\text{-}C_5Me_5)(OC)Ir[Os(CO)_4]_2$ (1*)

formula	$C_{19}H_{15}IrO_9Os_2$
fw	959.62
space group	$P\bar{1}$
cryst syst	triclinic
temp, °C	−78
a, Å	9.107 (3)
b, Å	9.128 (2)
c, Å	14.639 (2)
α, deg	84.63 (1)
β, deg	78.96 (2)
γ, deg	66.90 (2)
V, Å^3	1098.4
Z	2
d_{calcd}, g cm^{-3}	2.902
radiation, λ(Mo Kα), Å	0.71069 Å
μ(Mo Kα), cm^{-1}	176.2
cryst size, mm	0.16 × 0.32 × 0.38
scan method	ω–2θ
2θ range, deg	4–54
scan width (2θ), deg	0.85 + 0.35 tan θ
scan rate (2θ), deg min^{-1}	0.9–4.1
no. of unique data	4790
no. of obsd data ($I \geq 2.5\sigma(I)$)	3738
no. of variables	251
R^a	0.030
$R_w{}^b$	0.040[c]
GOF[d]	1.05

[a] $R = \sum||F_o| - |F_c||/\sum|F_o|$. [b] $R_w = [\sum w(|F_o| - |F_c|)^2/\sum(wF_o^2)]^{1/2}$. [c] $w = [54.425t_0(x) + 72.213t_1(x) + 22.807t_2(x)]^{-1}$ where $x = |F_o|/F_{max}$ and t_n are the polynomial functions of the Chebyshev series.[15] [d] $GOF = [\sum w(|F_o| - |F_c|)^2/(N_{observns} - N_{variables})]^{1/2}$.

cycle of refinement. The largest peak in the final difference map was 2.3 (0.3) e Å^{-3}, 0.87 Å from the iridium atom. An empirical weighting scheme was applied such that $\langle w(|F_o| - |F_c|)^2\rangle$ was nearly constant as a function of both $|F_o|$ and $(\sin\theta)/\lambda$.

Complex scattering factors for neutral atoms were used in the calculation of structure factors.[13] The computer programs used for data reduction, structure solution, and initial refinement were from the NRC VAX Crystal Structure System. The program suite CRYSTALS was employed in the final refinement of the structure.[14] All computations were performed on a MicroVAX-II computer. The final positional and isotropic or equivalent isotropic thermal parameters for the non-hydrogen atoms of 1* are given in Table II; bond lengths and selected angles for 1* are given in Table III. Other crystallographic data are deposited as supplementary material.

Results and Discussion

The clusters $(\eta^5\text{-}C_5R_5)(OC)Ir[Os(CO)_4]_2$ (R = H, 1; R = Me, 1*) were prepared in ~28% yield by the reaction of $(\eta^5\text{-}C_5R_5)Ir(CO)_2$ with $Os(CO)_4(\eta^2\text{-cyclooctene})$[11] in hexane at 55–65 °C (eq 1). Shore and co-workers prepared

$$Os(CO)_4(\eta^2\text{-cyclooctene}) + (\eta^5\text{-}C_5R_5)Ir(CO)_2 \xrightarrow{55\text{–}65\ ^\circ C} (\eta^5\text{-}C_5R_5)(OC)Ir[Os(CO)_4]_2 \quad (1)$$

R = H, 1; R = Me, 1*

$(\eta^5\text{-}C_5H_5)(OC)Rh[Os(CO)_4]_2$ (**1-Rh**) by the reaction of $Os_3(\mu\text{-}H)_2(CO)_{10}$ with $(\eta^5\text{-}C_5H_5)Rh(CO)_2$.[7] We attempted the preparation of 1* by the corresponding reaction of $Os_3(\mu\text{-}H)_2(CO)_{10}$ with $(\eta^5\text{-}C_5Me_5)Ir(CO)_2$ but were unsuccessful. Heating $Os(CO)_5$ and $(\eta^5\text{-}C_5Me_5)Ir(CO)_2$ together

Table II. Fractional Atomic Coordinates and Isotropic or Equivalent Isotropic Temperature Factors (Å^2) for 1*[a]

atom	x/a	y/b	z/c	U_{eq}/U_{iso}
Ir	0.98745 (4)	0.23716 (4)	0.20421 (2)	0.0212
Os(1)	0.76515 (4)	0.15795 (4)	0.33715 (3)	0.0229
Os(2)	0.70296 (4)	0.48321 (4)	0.28486 (2)	0.0212
O(11)	0.5695 (10)	0.1510 (10)	0.1890 (6)	0.0376
O(12)	0.9580 (9)	0.1820 (9)	0.4824 (5)	0.0361
O(13)	0.9690 (12)	−0.1973 (9)	0.3218 (8)	0.0494
O(14)	0.4821 (10)	0.1791 (10)	0.4914 (6)	0.0437
O(21)	0.5606 (12)	0.4743 (10)	0.1118 (6)	0.0449
O(22)	0.8563 (9)	0.5226 (9)	0.4463 (5)	0.0344
O(23)	0.3748 (10)	0.6079 (11)	0.4097 (7)	0.0470
O(24)	0.7320 (13)	0.7928 (10)	0.2074 (6)	0.0462
O(31)	0.8522 (10)	0.1766 (13)	0.0490 (6)	0.0394
C(1)	1.2276 (10)	0.1198 (12)	0.2636 (7)	0.0217
C(2)	1.2411 (11)	0.0629 (12)	0.1745 (8)	0.0295
C(3)	1.2154 (11)	0.1930 (14)	0.1100 (8)	0.0314
C(4)	1.1794 (11)	0.3351 (12)	0.1600 (8)	0.0286
C(5)	1.1853 (11)	0.2867 (12)	0.2572 (7)	0.0275
C(6)	1.2761 (13)	0.0139 (15)	0.3473 (8)	0.0401
C(7)	1.2956 (16)	−0.1098 (14)	0.1497 (10)	0.0436
C(8)	1.2397 (15)	0.1850 (20)	0.0063 (8)	0.0471
C(9)	1.1608 (16)	0.4960 (16)	0.1182 (12)	0.0463
C(10)	1.1950 (13)	0.3860 (14)	0.3287 (10)	0.0397
C(11)	0.6410 (12)	0.1569 (12)	0.2420 (7)	0.0302 (20)
C(12)	0.8918 (12)	0.1762 (12)	0.4262 (7)	0.0300 (20)
C(13)	0.8935 (13)	−0.0657 (13)	0.3272 (8)	0.0361 (23)
C(14)	0.5858 (12)	0.1722 (12)	0.4345 (7)	0.0295 (20)
C(21)	0.6185 (13)	0.4683 (12)	0.1749 (7)	0.0340 (21)
C(22)	0.8083 (12)	0.4978 (11)	0.3877 (7)	0.0294 (20)
C(23)	0.4955 (12)	0.5610 (12)	0.3631 (7)	0.0301 (20)
C(24)	0.7222 (12)	0.6754 (12)	0.2351 (7)	0.0312 (20)
C(31)	0.8925 (13)	0.2033 (13)	0.1118 (7)	0.0349 (22)

[a] $U_{eq} = (1/3)\sum_i\sum_j U_{ij}a_ia_ja_ia_j$.

Table III. Bond Lengths and Selected Angles for 1*

Bond Lengths, Å			
Ir–Os(1)	2.7902 (5)	C(12)–O(12)	1.13 (1)
Ir–Os(2)	2.8124 (5)	C(13)–O(13)	1.13 (1)
Os(1)–Os(2)	2.8536 (5)	C(14)–O(14)	1.12 (1)
Ir–C(1)	2.324 (8)	C(21)–O(21)	1.14 (1)
Ir–C(2)	2.217 (9)	C(22)–O(22)	1.11 (1)
Ir–C(3)	2.17 (1)	C(23)–O(23)	1.12 (1)
Ir–C(4)	2.227 (9)	C(24)–O(24)	1.14 (1)
Ir–C(5)	2.301 (9)	C(31)–O(31)	1.23 (1)
Ir–C(31)	1.85 (1)	C(1)–C(2)	1.42 (1)
Os(1)–C(11)	1.96 (1)	C(1)–C(5)	1.42 (1)
Os(1)–C(12)	1.96 (1)	C(1)–C(6)	1.51 (1)
Os(1)–C(13)	1.92 (1)	C(2)–C(3)	1.42 (2)
Os(1)–C(14)	1.92 (1)	C(2)–C(7)	1.51 (1)
Os(2)–C(21)	1.95 (1)	C(3)–C(4)	1.44 (2)
Os(2)–C(22)	1.97 (1)	C(3)–C(8)	1.50 (2)
Os(2)–C(23)	1.91 (1)	C(4)–C(5)	1.45 (1)
Os(2)–C(24)	1.90 (1)	C(4)–C(9)	1.50 (1)
C(11)–O(11)	1.12 (1)	C(5)–C(10)	1.48 (1)
Angles (deg)			
Os(2)–Ir–Os(1)	61.24 (1)	C(3)–Ir–C(2)	37.7 (4)
Os(2)–Os(1)–Ir	59.77 (1)	C(4)–Ir–C(1)	61.2 (3)
Os(1)–Os(2)–Ir	59.00 (1)	C(4)–Ir–C(2)	63.0 (4)
C(2)–C(1)–C(6)	124.2 (9)	C(4)–Ir–C(3)	38.2 (4)
C(5)–C(1)–C(6)	126.2 (9)	C(5)–Ir–C(1)	35.7 (3)
C(5)–C(1)–C(2)	109.0 (9)	C(5)–Ir–C(2)	61.3 (3)
C(1)–C(2)–C(7)	125.9 (10)	C(5)–Ir–C(3)	62.4 (4)
C(3)–C(2)–C(7)	125.5 (11)	C(5)–Ir–C(4)	37.4 (4)
C(3)–C(2)–C(1)	108.2 (9)	C(12)–Os(1)–C(11)	174.7 (4)
C(2)–C(3)–C(8)	126.7 (12)	C(13)–Os(1)–C(11)	93.2 (4)
C(4)–C(3)–C(8)	124.4 (11)	C(13)–Os(1)–C(12)	90.3 (4)
C(4)–C(3)–C(2)	108.5 (9)	C(14)–Os(1)–C(11)	91.2 (4)
C(3)–C(4)–C(9)	126.3 (11)	C(14)–Os(1)–C(12)	91.6 (4)
C(5)–C(4)–C(9)	126.8 (11)	C(14)–Os(1)–C(13)	104.5 (4)
C(5)–C(4)–C(3)	106.5 (9)	C(22)–Os(2)–C(21)	174.3 (4)
C(1)–C(5)–C(10)	125.7 (10)	C(23)–Os(2)–C(21)	94.7 (4)
C(4)–C(5)–C(10)	124.1 (10)	C(23)–Os(2)–C(22)	90.7 (4)
C(4)–C(5)–C(1)	107.8 (9)	C(24)–Os(2)–C(21)	89.1 (4)
C(2)–Ir–C(1)	36.2 (4)	C(24)–Os(2)–C(22)	88.0 (4)
C(3)–Ir–C(1)	61.3 (4)	C(24)–Os(2)–C(23)	101.6 (4)

(13) *International Tables for X-ray Crystallography*; Kynoch Press: Birmingham, England, 1975; Vol. IV, p 99.

(14) (a) Gabe, E. J.; Larson, A. C.; Lee, F. L.; Le Page, Y. NRC VAX Crystal Structure System; Chemistry Division, National Research Council: Ottawa, Canada, 1985. (b) Watkin, D. J.; Carruthers, J. R.; Betteridge, P. W. *CRYSTALS*; Chemical Crystallography Laboratory, University of Oxford: Oxford, England, 1985.

(15) Carruthers, J. R.; Watkin, D. J. *Acta Crystallogr., Sect. A: Cryst. Phys., Diffr., Theor. Gen. Crystallogr.* **1979**, *A35*, 698.

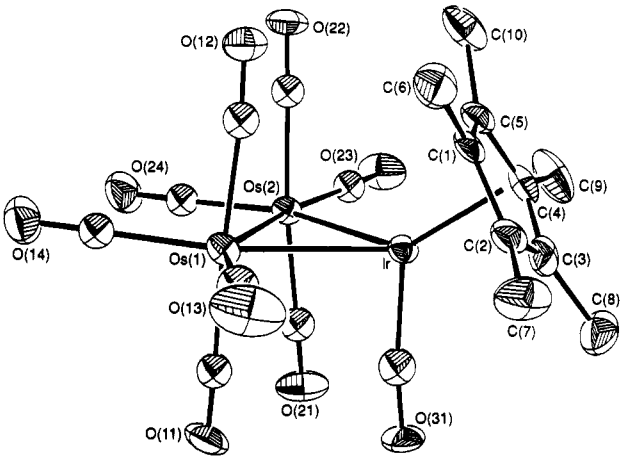

Figure 1. Molecular structure of $(\eta^5\text{-}C_5Me_5)(OC)Ir[Os(CO)_4]_2$ (**1***).

in hexane also failed to produce **1***. We have, however, observed **1*** in trace amounts in the prolonged reaction of $Os_3(CO)_{10}$(cyclooctene)$_2$ with $(\eta^5\text{-}C_5Me_5)Ir(CO)_2$. Presumably **1*** results from the disintegration of a tetranuclear cluster (we have isolated $(\eta^5\text{-}C_5Me_5)IrOs_3(CO)_{12}$ from the same reaction[16]). The last reaction therefore resembles the formation of **1*-Rh** from $Os_2(\mu\text{-}\eta^1,\eta^1\text{-}CH_2CH_2)(CO)_8$ and $[Rh(\mu\text{-}CO)(\eta^5\text{-}C_5Me_5)]_2$[8] and represents further evidence of the instability of clusters with four unsupported metal–metal bonds.[17]

Like **1-Rh** and **1*-Rh**, the iridium analogues are deep red, air-stable, crystalline solids. The infrared spectra in the carbonyl region of **1** and **1*** are similar to those reported by Washington and Takats for **1-Rh**, and **1*-Rh**.[8] There is no evidence in the spectra for bridging carbonyls.

Structure of 1*. A view of the molecule is shown in Figure 1; bond lengths and selected angles are given in Table III. As can be seen from Figure 1, **1*** may be regarded as derived from $Os_3(CO)_{12}$[18] in which one of the $Os(CO)_4$ units has been replaced by the isolobal fragment $Ir(\eta^5\text{-}C_5Me_5)(CO)$. The carbonyl ligand on the iridium atom occupies an axial site. The structure of **1*** is similar to that of **1-Rh** except that the orientations of the cyclopentadienyl rings are slightly different: in **1***, two carbon atoms (C(1), C(5)) of the ring carbons are closest to the osmium atoms, whereas in **1-Rh** only one carbon atom of these carbons is closest to these metal atoms.[7] Both molecules have close to (but not exact) mirror symmetry in the solid state. The Os–Os bond length in **1*** of 2.8536 (5) Å may be compared to 2.8455 (4) Å, the Os–Os bond length in **1-Rh**,[7] and 2.877 Å, the average Os–Os bond length in $Os_3(CO)_{12}$.[18] The Os–Ir bond lengths in **1*** (2.7902 (5) and 2.8124 (5) Å) are in the range 2.776 (5)–2.881 (1) Å previously found for single, unbridged Os–Ir bonds in cluster compounds.[19] As in $Os_3(CO)_{12}$,[18] the axial Os–C bonds (average length = 1.96 Å) are longer than the equatorial Os–C bonds (average length = 1.91 Å). The geometry about the $Os_2(CO)_8$ unit in **1*** is closely similar to those of the $Os_2(CO)_8$ units in $Os_3(CO)_{12}$. The nearest nonbonding distances of a carbonyl carbon to a metal atom are Ir–C(12) = 3.25 (1), Ir–C(21) = 3.28 (1), and Os(1)–C(31) = 3.32 (1) Å.

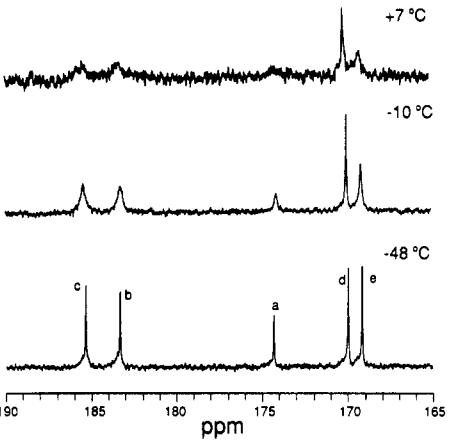

Figure 2. Variable-temperature ^{13}C NMR spectra of **1** in CH_2Cl_2/CD_2Cl_2 (^{13}CO-enriched sample; 100.6-MHz operating frequency).

Chart I

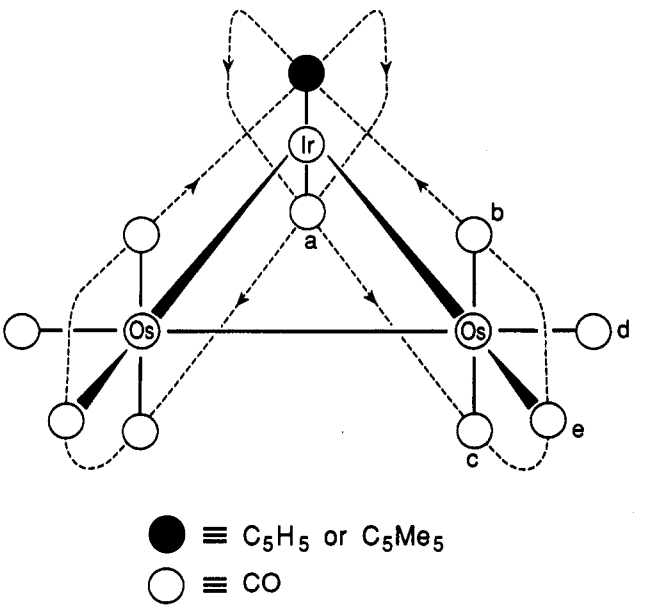

Carbonyl Exchange in 1 and 1*. The ^{13}C NMR spectrum of ^{13}CO-enriched **1** in CH_2Cl_2/CD_2Cl_2 at −48 °C exhibits five carbonyl resonances in the ratio 2:2:1:2:2 (Figure 2). The assignment of the resonances shown in Figure 2 and Chart I is based on the following arguments. The signal of intensity 1 at δ 174.3 is unambiguously assigned to the carbonyl on iridium on the basis of intensity; it also appears in the region associated with carbonyl ligands bound to iridium.[20] The two resonances to low field of this signal at δ 185.3 and 183.4 are attributed to the two types of axial carbonyls on osmium. In saturated trinuclear clusters of osmium, the signals due to axial carbonyls invariably come to low field to those of the equatorial carbonyls.[5,20,21] There was also evidence in the spectrum at −33 °C (not shown) that these signals exhibit ^{13}C–^{13}C coupling as expected for a trans arrangement of two carbonyls that are chemically different.[22] (The level of ^{13}CO

(16) Johnston, V. J.; Einstein, F. W. B.; Pomeroy, R. K. *J. Am. Chem. Soc.* **1987**, *109*, 7220.
(17) (a) Johnston, V. J.; Einstein, F. W. B.; Pomeroy, R. K. *J. Am. Chem. Soc.* **1987**, *109*, 8111. (b) Lauher, J. W. *Int. J. Quantum Chem., Quantum Chem. Sym.* **1988**, *22*, 309. (c) Mealli, C.; Proserpio, D. M. *J. Am. Chem. Soc.* **1990**, *112*, 5484.
(18) Churchill, M. R.; DeBoer, B. G. *Inorg. Chem.* **1977**, *16*, 878.
(19) Johnson, B. F. G.; Lewis, J.; Raithby, P. R.; Azman, S. N.; Syed-Mustaffa, B.; Taylor, M. J.; Whitmire, K. H.; Clegg, W. *J. Chem. Soc., Dalton Trans.* **1984**, 2111.
(20) Mann, B. E.; Taylor, B. F. *^{13}C NMR Data for Organometallic Compounds*; Academic: New York, 1981; pp 176 and 180.
(21) Aime, S.; Osella, D.; Milone, L.; Rosenberg, E. *J. Organomet. Chem.* **1981**, *213*, 207.
(22) (a) Tachikawa, M.; Richter, S. I.; Shapley, J. R. *J. Organomet. Chem.* **1977**, *128*, C9. (b) Aime, S.; Osella, D. *J. Chem. Soc., Chem. Commun.* **1981**, 300.

enrichment used in the sample was approximately 30%.) The resonance at δ 185.3 is tentatively assigned to the carbonyls labeled c in the chart on the basis that the resonances due to the carbonyls on the opposite side of the Os_2Ir plane to that occupied by the cyclopentadienyl ligand should be less affected on going from 1 to 1*. (In 1* the resonances of carbonyls b and c are degenerate and occur at δ 185.9.) The two highest field signals, at δ 169.9 and 169.1, are assigned to carbonyls d and e, respectively, on the basis of the exchange mechanism proposed below. The signals are in the region expected for equatorial carbonyls of $Os(CO)_4$ groupings in trinuclear clusters.[5,20,21] The changes in the chemical shifts of the signals due to carbonyls d and e on going to 1* are consistent with the argument used above to assign the resonances attributed to carbonyls b and c.

The presence of two signals for the axial carbonyls of the $Os(CO)_4$ units indicates the $Ir(\eta^5\text{-}C_5H_5)(CO)$ unit is rigid in 1 at −48 °C. Because of CO exchange (described below), it is impossible to ascertain from the NMR evidence whether the Ir unit rotates with respect to the $Os_2(CO)_8$ moiety at higher temperatures.

On warming the sample of 1 to +7 °C, four of the carbonyl resonances collapse to the base line (Figure 2). This behavior is interpreted in terms of partial merry-go-round CO exchanges that take place in those planes that are perpendicular to the plane containing the metal atoms and that pass through the iridium and one of the osmium atoms. The exchanges are illustrated in Chart I. Complete merry-go-round CO exchanges have been proposed many times before to account for the coalescences of resonances in the variable-temperature ^{13}C NMR spectra of metal carbonyl cluster and binuclear compounds.[23-27] It is only a partial merry-go-round in 1 since the cyclopentadienyl ligand remains coordinated to the iridium atom. For this reason, the mechanism requires that CO exchange takes place alternatively in the two planes so that the C_5H_5 group is always coordinated to the two equatorial sites on iridium but rocks back and forth between the two axial sites as each successive CO exchange occurs. After six individual exchanges, each carbonyl of type a, b, c, or e has visited each one of the other chemically different sites in this group of carbonyls. The signals assigned to carbonyls a, b, c, and e should therefore coalesce to a singlet. This is observed for 1* (see below) and for 1-**Rh**, where the same mechanism of CO exchange has been proposed.[8] The carbonyls labeled d do not take part in these exchanges (Chart I), and consequently, the signal attributed to these carbonyls remains sharp as the exchanges become fast on the NMR time scale, as observed. This is, however, more clearly seen in the spectra of 1* (and 1-**Rh**).

As pointed out by a referee, the proposed exchange process leads to the following specific site exchanges in one plane: a → b, b → a, c → e, e → c. However, since the Cp ring moves from above to below the Os_2Ir plane, the other set of carbonyls labeled b and c also exchange, whereas the remaining carbonyl labeled e is unchanged.

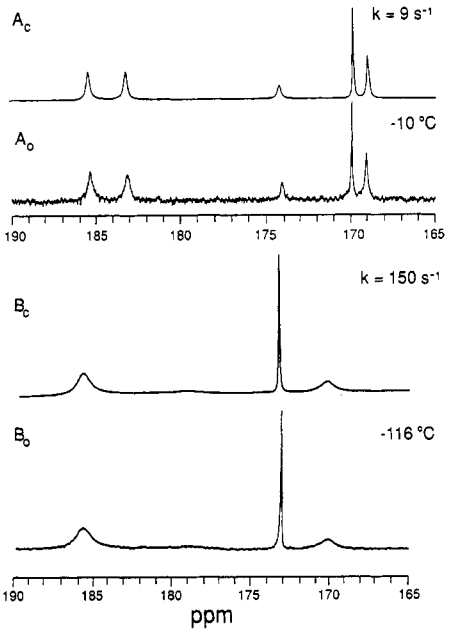

Figure 3. Calculated (A_c) and observed (A_o) ^{13}C NMR spectra for 1 at −10 °C; calculated (B_c) and observed (B_o) ^{13}C NMR spectra for 1* at −116 °C.

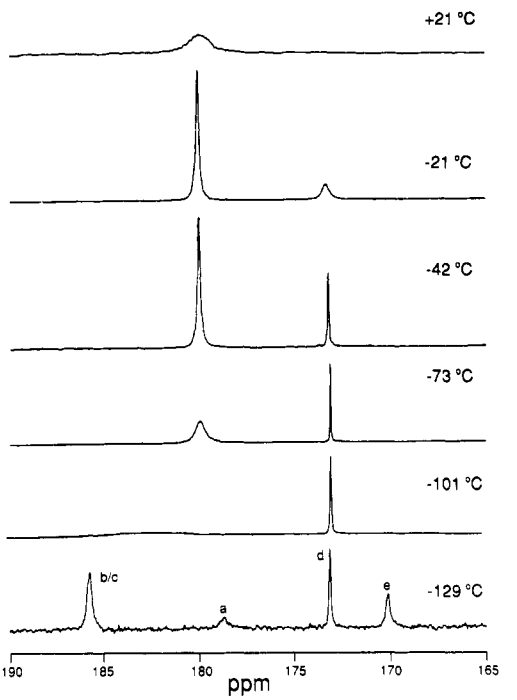

Figure 4. Variable-temperature ^{13}C NMR spectra of 1* in CH_2Cl_2/CD_2Cl_2 except spectrum at −129 °C (in $CHFCl_2/CD_2Cl_2$).

If the rate of loss of spins from site a is k (s^{-1}), then it is also k from site e, but $2k$ from sites b and c. Since the amount of initial line broadening is proportional to the total rate of spin loss, the resonances attributed to carbonyls b and c should broaden faster than those due to carbonyls a and e. This is seen in the spectrum at −10 °C (Figure 2). (Both k and $2k$ were used in the simulations shown in Figure 3.)

In $Os_3(CO)_{11}(PR_3)$ clusters, merry-go-round CO exchanges are believed to occur in the two planes that are perpendicular to the Os_3 plane and that pass through two of the metal atoms, but not through the phosphorus atom. In a similar manner to 1 (and 1*), one carbonyl does not take part in the exchanges, and the ^{13}C NMR resonance due to this carbonyl in the variable-temperature ^{13}C NMR

(23) Cotton, F. A.; Hunter, D. L. *Inorg. Chim. Acta* **1974**, *11*, L9.
(24) Johnson, B. F. G.; Lewis, J.; Reichert, B. E.; Schorpp, K. T. *J. Chem. Soc., Dalton Trans.* **1976**, 1403.
(25) Deeming, A. J.; Donovan-Mtunzi, S.; Kabir, S. E.; Manning, P. J. *J. Chem. Soc., Dalton Trans.* **1985**, 1037. See also ref 2b, pp 47–48.
(26) Adams, H.; Bailey, N. A.; Bentley, G. W.; Mann, B. E. *J. Chem. Soc., Dalton Trans.* **1989**, 1831.
(27) For example: (a) Adams, R. D.; Cotton, F. A. *J. Am. Chem. Soc.* **1973**, *95*, 6589. (b) Schmidt, S. P.; Basolo, F.; Jensen, C. M.; Trogler, W. C. *J. Am. Chem. Soc.* **1986**, *108*, 1894. (c) Kiel, G.-Y.; Takats, J. *Organometallics* **1989**, *8*, 839. (d) Davis, H. B.; Einstein, F. W. B.; Glavina, P. G.; Jones, T.; Pomeroy, R. K.; Rushman, P. *Organometallics* **1989**, *8*, 1030.

spectra of these clusters remains sharp as the other resonances collapse.[5,25]

Simulation of the spectrum of 1 at −10 °C (Figure 3A) gave a rate constant for the CO exchange (i.e., k) of 9 ± 1 s^{-1} which corresponds to a $\Delta G^{\ddagger}$ of 14.2 ± 0.3 kcal mol^{-1} for the process, at −10 °C. This value may be compared to a $\Delta G^{\ddagger}$ of 8.4 ± 0.4 kcal mol^{-1}, the value found for the corresponding process in **1-Rh** (at −80 °C).[8] As mentioned in the Introduction, it is generally found that the barrier to carbonyl exchange in metal cluster compounds increases on going to the metal atom lower in the periodic table; the pair of molecules 1 and **1-Rh** illustrate this effect.

Variable-temperature ^{13}C NMR spectra of ^{13}CO-enriched 1* in CH_2Cl_2/CD_2Cl_2 are shown in Figure 4. The assignment of the signals is based on similar arguments to those used in the assignment of the signals in 1; note that the resonances attributed to the axial carbonyls on the $Os(CO)_4$ units in 1* are degenerate.

As can be seen from Figures 2 and 4, there is a dramatic lowering of the barrier to carbonyl exchange in 1* compared to that in 1. Even with the sample of 1* at −129 °C, the carbonyl resonances are still somewhat broadened due to exchange. With the line width parameter used in the simulation of the spectrum of 1 (Figure 3A), it was possible to simulate the spectrum of 1* at −116 °C (Figure 3B). This yielded a rate constant of 150 ± 15 s^{-1}, which in turn gave a $\Delta G^{\ddagger}$ of 7.4 ± 0.2 kcal mol^{-1} for the carbonyl exchange in 1* at −116 °C.

The difference of 6.8 kcal mol^{-1} in the activation barriers to carbonyl exchange is remarkable. A similar difference was observed in the variable-temperature ^{13}C NMR spectra of **1-Rh** and **1*-Rh**.[8] The exchange of the carbonyls a, b, c, and e in **1*-Rh** at −100 °C, was, however, so fast that a sharp singlet was still observed for these carbonyls. As found for **1-Rh** and **1*-Rh**, the ^{13}C NMR spectra indicate that when 1 and 1* are undergoing CO exchange at a comparable rate the temperature of the sample of 1 is some 100 °C higher than that of the sample of 1*.

A similar, although not so dramatic, effect is observed in the barrier to carbonyl exchange in $Os_3(CO)_{11}[P(OMe)_3]$ compared to that in $Os_3(CO)_{12}$: in the phosphite derivative, the barrier to the merry-go-round CO exchange in the plane that is perpendicular to the Os_3 plane and passes through the three carbonyls of the $Os(CO)_3[P(OMe)_3]$ was found to be 14.0 ± 0.4 kcal mol^{-1} at 20 °C.[5] The barrier to axial–equatorial carbonyl exchange in $Os_3(CO)_{12}$ has been estimated as 16.3 kcal mol^{-1} at 20 °C.[28] In order to rationalize these results, it was reasoned that substitution of the carbonyl ligand in $Os_3(CO)_{12}$ by $P(OMe)_3$ would increase the electron density at the osmium atom where substitution had occurred, since $P(OMe)_3$ is a better donor ligand than CO. The increase in the electron density would cause expansion of the 5d orbitals on the osmium atom. This in turn could result in better overlap with the π^* orbitals of the axial carbonyls on the adjacent osmium atom and thus lower the activation energy needed to form the intermediate with bridging carbonyls.[5] Similar arguments may be used to rationalize the much lower barrier to carbonyl exchange in 1* compared to that in 1.

As the temperature of 1* was raised above −42 °C, the signal assigned to the carbonyls labeled d (Chart I) broadened and collapsed to the base line as did, at a slower rate, the averaged signal due to the other carbonyls (Figure 4). This indicates that the carbonyls labeled d are now exchanging with the carbonyls designated a, b, c, and e. Although there are several mechanisms that can account for this behavior, we believe the most probable is a (complete) merry-go-round CO exchange that occurs in the plane that is perpendicular to the Os_2Ir plane and passes through the two osmium atoms. As mentioned previously, this type of mechanism has been proposed to account for the CO exchange in other trinuclear osmium clusters. As expected, the barrier to this exchange is less sensitive to the third metal atom in the cluster (e.g., Os[5,25] Rh,[8] or Ir) and the substituents on the third metal atom.

Acknowledgment. The financial support of Natural Sciences and Engineering Research Council of Canada (to F.W.B.E and R.K.P.) and the Swiss National Science Foundation (to A.R.) is gratefully acknowledged. We also thank Professor J. Takats (University of Alberta) for a copy of Dr. M. R. Burke's Ph.D. thesis and the referees for helpful comments.

Supplementary Material Available: Tables of fractional coordinates and thermal parameters for the hydrogen atoms and anisotropic temperature factors for 1* (1 page); listings of observed and calculated structure factors for 1* (33 pages). Ordering information is given on any current masthead page.

(28) Ma, A. K.; Pomeroy, R. K. Unpublished results. See also: (a) Forster, A.; Johnson, B. F. G.; Lewis, J.; Matheson, T. W.; Robinson, B. H.; Jackson, W. G. *J. Chem. Soc., Chem. Commun.* **1974**, 1042. (b) Aime, S.; Gambino, O.; Milone, L.; Sappa, E.; Rosenberg, E. *Inorg. Chim. Acta* **1975**, *15*, 53.